

Determining heat flow of engineering metals in steady state conduction

Robert Hawken

School of Engineering, University of the Sunshine Coast.

1 Introduction

The nature of metallic atomic bonding varies greatly between polymers and ceramics due to the 'sea of electrons' available for electrical and thermal conduction in metals. The amount of available electrons for either electrical or thermal conduction is determined by the arrangement of valance electrons in the most outer electron shell (Callister 2018).

Thermal conduction in metals is determined by the process of electron collisions, by passing high vibrational energy along a temperature gradient and which is denoted as k (Askeland and Wright 2016). The efficiency of electron motion is determined by the arrangement of electrons, impurities and material properties between alloys (Callister 2018).

Due to the nature of steady state thermal conduction appearing as a wave, it is possible to measure the heat flow through materials between two known points. Fourier's law of heat conduction is used to describe the relationships between each parameter (Cengel and Ghajar 2015). The heat flow rate is directly proportional to the thermal conductivity value, cross sectional area and temperature difference and inversely proportional to the distance the heat flow travels (Cengel and Ghajar 2015).

Understanding thermal conductivity is paramount for many engineering applications as the rate of heat flow through a material can be measured to manage thermal safety and operational requirements (Askeland and Wright 2016).

With respect to the previous foundations of steady heat conduction, it is hypothesised that materials with higher thermal conductivity values will have decreased time when measuring temperature change over a known distance. These findings will be used to verify the current implementation of thermal conduction management in engineering heat transfer and material science.

1.1 Governing Equations

The primary equations used for this experiment is Fourier's Law of Heat Conduction. This formula is derived from a partial differential equation and can be used to find the rate of heat flow in Joules per second, with known thermal conductivity, material cross sectional area, change in temperature and known distance of heat transfer.

$$\frac{\Delta Q}{\Delta t} = \frac{k \cdot A \cdot \Delta T}{0.030} \quad (1)$$

The heat pulse can be calculated by the distance over the time taken for thermal conduction to occur.

$$\vec{v}\left(\frac{m}{s}\right) = \frac{\Delta x(m)}{\Delta t(s)} \quad (2)$$

2 Experimental Design

2.1 Conduction Race Methods and Materials

A TD-8513 thermal conduction kit was used with material samples of 6063-T5 Aluminium ($90 \cdot 12 \cdot 4$ mm), 304 Stainless Steel ($90 \cdot 12 \cdot 4$ mm) and two 360-alloy Brass samples with different widths ($90 \cdot 12 \cdot 4$ mm & $90 \cdot 7 \cdot 4$ mm). In Heat mode, the TD-8513 device was subjected to 5V DC power supply with a temperature sampling rate of 5Hz for 5 minutes. Insulating foam was placed over the material samples to reduce convection (Figure 1). The temperature and time at each thermistor was recorded with the provided software and processed in MATLAB (Figures 2, 3 & 4).

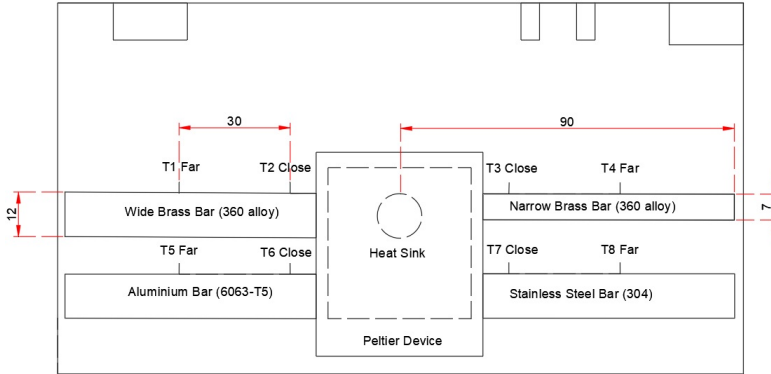


Figure. 1: Peltier Device TD-8513 with Thermistors placed 30mm apart

2.2 Heat Pulse Methods

Following the same power and initial procedure in section 2.1, the temperature sampling rate was set to 2Hz once the samples returned to room temperature. Once the temperature of T2 reached 40° the Peltier device was changed from Heat mode to Cool mode each 30 seconds for 5 minutes. Temperature difference between close and far thermistors was recorded and presented in Figure 4 & 5.

2.3 Numerical Analysis

PASCO manufactures provide thermal conductivity values for the engineering materials based on each specific alloy. Graphical illustrations of collected data and gradient of tangent lines denoting rate of temperature change was completed using MATLAB 2022Ra edition. Heat Flow rate and Heat Pulse for each engineering material 30mm apart was calculated using Microsoft Excel 365.

3 Results and Discussion

3.1 Conduction Race (*Following methods from section 2.1*)

The temperature recordings from the 'far' thermistors of each engineering material is displayed in Figure 2. The most efficient heat conductor is Aluminium at Thermistor position T5, reaching 40 degrees after 5 minutes.

In the first 50 seconds, the gradient of temperature change of aluminium was 0.17, this is due to the relatively high thermal conductivity rating of Aluminium 6063-T5 is $150(\frac{W}{m \cdot K})$ (Bluesea 2019).

The least efficient heat conductor is Stainless Steel at Thermistor position T8. In the first 50 seconds, the gradient of the temperature change was 0.003. This difference results in Aluminium increasing temperature at 55 fold faster than Stainless Steel (Figure 2) over the 30mm span.

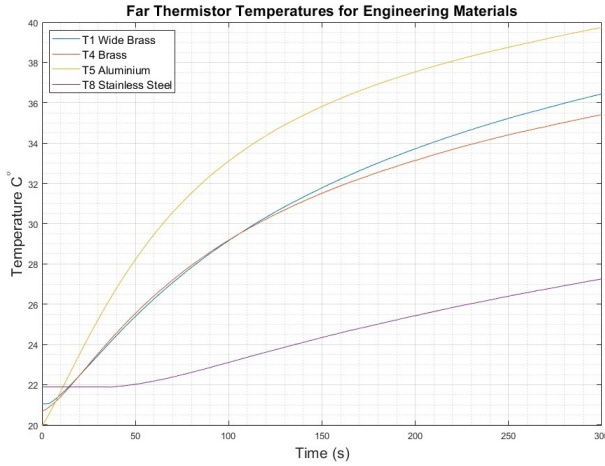


Figure. 2: Temperatures from Far Thermistors for Engineering materials

Minimal gradient differences were observed between Brass samples. The 12mm wide sample experienced the higher overall temperature, however less than one degree Celsius difference after 5 minutes (Figure 2). Following the properties of Fourier's Law of Heat conduction (Eq. 1), it is evident that heat flow is time and distance dependent (Chung, 2001). In the Wide Brass sample, it took 3.2 seconds for the temperature in the far thermistor (T2) to register temperature change (Figure 3). Equation 2 results in a Wide Brass heat pulse of $9.4(\frac{mm}{s})$.

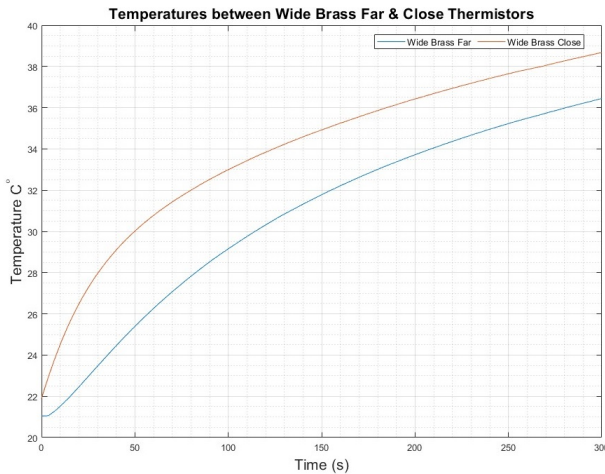


Figure. 3: Wide Brass Temperatures from Close and Far Thermistors

To further understand the relationships of material properties, thermal conductivity and heat flow rate, it is important to compare the temperature change between thermistors within the same sample (Figure 4) (Chung, 2001).

Stainless Steel observed the highest overall temperature difference $\approx 9^\circ$, which in fact had properties similar to a thermal insulator (Figure 4) (Cengel and Ghajar 2015). Thermal energy takes longer to arrive at the far thermistor due to the 30mm distance (Ozis and Tzou, 1994). Aluminium had the smallest temperature difference over the 30mm distance $\approx 0.9^\circ$ and therefore was the most efficient thermal conductor (Figure 4). This correlation is evident following the material property tables (Table 1) [AZoM (2019), Brass 360 (2022), Eng Toolbox (2019), Pasco (2022)].

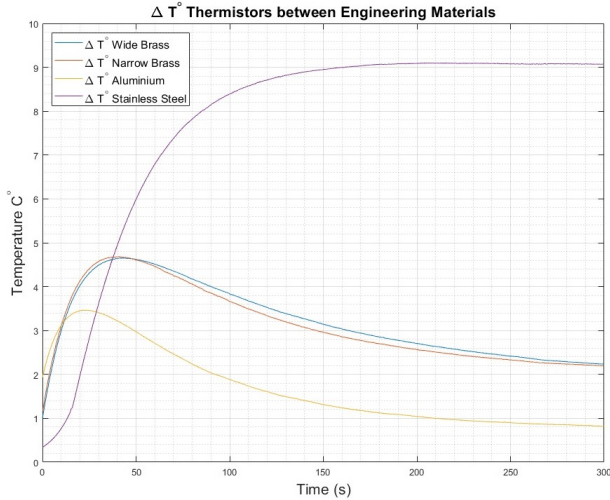


Figure. 4: Δ Temperature of Close and Far Thermistors for each Metal

Table 1 indicates that Aluminium is the most pure substance with 97.5% whereas both brass and Stainless Steel samples are $\approx 60\%$ alloy. This verifies the high thermal conductivity of Aluminium, however it has the lowest heat flow rate of 0.28 (J/s) (Equation 1). These values indicate that Aluminium does conduct heat faster, however it is not able to transfer as much total heat transfer compared to the other materials (Ozis and Tzou, 1994).

Table 1: Material properties & Heat flow rate \dot{Q}

Property	Wide Brass	Narrow Brass	Aluminium	Stainless Steel
Primary Composition %	61 Cu	61 Cu	97.5 Al	58 Fe
Secondary Composition %	35 Zn	35 Zn	0.5 Mg	18 Cr/ 10 Ni
Thermal Conductivity	115	115	150	14
Heat Flow Rate	0.368	0.24	0.26	0.201
Published Heat Flow Rate	0.36	0.28	0.28	0.17
Error	2.2%	-14%	-7.14%	15.7%

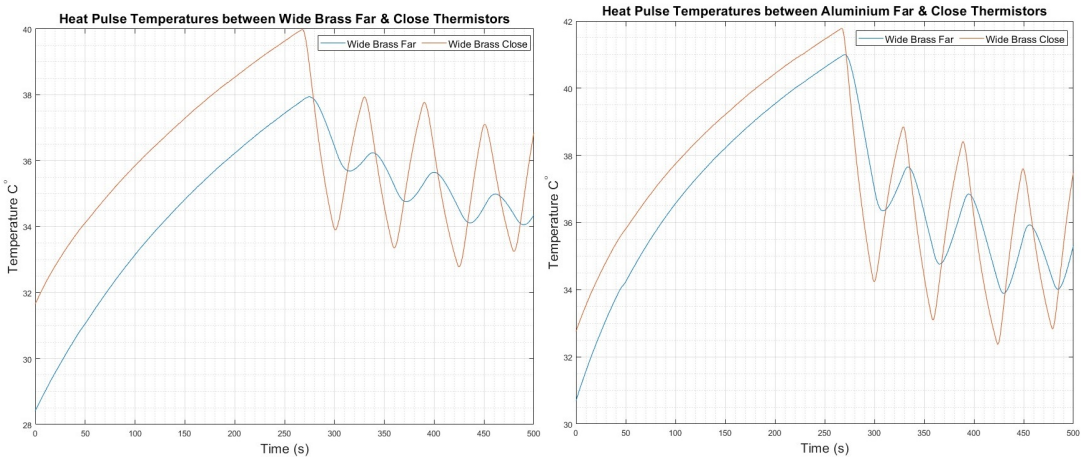
It is evident that cross sectional area of the sample does effect Heat flow rate between 12mm and 7mm Brass width samples (Table 1) (Equation 1). The narrow sample has 58% less cross sectional area, which transposes to a 24% reduction in heat flow rate, however both brass samples result in $\approx 2.2^\circ$ temperature difference equilibrium (Figure 4).

The initial peak of temperature difference arises due to the thermal conduction arising at the close thermistor which produces a large initial temperature difference (Pasco 2022). As time increases, the far thermistor receives more thermal energy and therefore finds an equilibrium point stated above (Figure 4).

Minimal error was observed between experimental and published data (Pasco 2022)(Table 1). The heat flow rates were higher in Narrow Brass and Aluminium and lower in Stainless Steel. This could be due to measurement differences and change in ambient temperature with the published data (Figure 4) (Pasco 2022).

3.2 Heat Pulse (*Following methods from section 2.2*)

Figure 5a, suggests the close thermistor at position T2 records temperature change more frequently with higher peaks and troughs experienced than at T1. The average time between close and far peaks is 9 seconds with an average temperature difference of 2.11° (Figure 5a) (Equation 2). This relationship is due to the aforementioned time required for the heat flow to pass through the sample.



(a) *Wide Brass Heat Pulse* (b) *Aluminium Heat Pulse*
Figure. 5: Wide Brass and Aluminium Temperatures during 30s cyclic heat pulse.

Figure 5b indicates the temperature changes due to the cyclic hot and cool functions in a similar manner as for wide brass. It is evident that Aluminium is a more efficient thermal conductor, due to the reduced vertical phase shift between each thermistor reading (Figure 5b). This concept is further reinforced as there was a greater amplitude change in the Aluminium sample during each cycle. The average time difference between aluminium thermal amplitudes is 6.5 seconds with a 1.48° average temperature difference (Figure 5).

This results in a 27% faster thermal conduction between thermistors with a 30% reduction in temperature difference between thermistors. Ozis and Tzou (1994) describes these changes in amplitude as the opposite flow of current, which cancels the positive and negative portions of the wave, resulting in a mean display. This is one wave however the direction of conduction is displayed as two (Ozis and Tzou 1994).

Thermal conductivity is a materials predisposition to conduct heat through the electron transport while heat flow rate is the amount and speed of heat energy at which the thermal conductivity occurs. Heat flow rate is effected by the surface area and distance the thermal energy travels (Cengel and Ghajar 2015). Hence why Wide Brass has a higher heat flow rate than Aluminium (Table 1). However the Aluminium conducts heat at a faster rate due to it's high thermal conductivity, which is a material property and is effected by temperature (Figure 4)(Cengel and Ghajar 2015).

3.3 Error and Recommendations

The primary recommendation would involve testing thermal conduction at different initial temperatures. It is a well known fact that thermal conductivity changes with a change in temperature. Liquid nitrogen can be used to reduce initial temperatures to -196°

It is also recommended for future studies to obtain different metals and alloys to broaden the array of tested materials. As Brass is a copper alloy, it would be interesting to measure thermal conductivity against pure copper.

4 Conclusion

In conclusion, the thermal conductivity properties and heat flow measurements have been verified with respect to the published data surrounding these specific metal alloys. It was hypothesized that materials with higher thermal conductivity values will have decreased time when measuring temperature change over a known distance. This relationship has been discovered in multiple experimental designs in both steady state conduction and oscillating steady state conduction.

As stated, Equation 1 indicates the relationship between thermal conductivity, temperature change and cross sectional area. The narrow brass sample resulted in a reduced heat flow, while maintaining the same thermal conductivity. It was seen that due to the alloy components of Stainless Steel, the inclusion of Chromium and Nickel reduces the available electrons for heat transfer compared to near pure Aluminium.

These results are concurrent with the literature in relation to thermal conduction and heat flow in the TD-8513 experimental protocol. This data will be used in engineering practice and material science to verify the current applications and understanding of thermal conductivity in metals.

References

1. Askeland, D.R., Fulay, P.P. and Wright, W.J. (2011). The science and engineering of materials. Stamford, Ct: Cengage Learning.
2. ASM Material Data Sheet. (2022) [online] Available at: <https://asm.matweb.com/search/SpecificMaterial.asp?bassnum=MA6063T5> [Accessed 29 May 2022].
3. AZoM (2019). Stainless Steels - Stainless 304 Properties, Fabrication and Applications. [online] AZoM.com. Available at: <https://www.azom.com/article.aspx?ArticleID=2867>.

4. Bluesea.com. (2019). Electrical Conductivity of Materials - Blue Sea Systems. [online] Available at: [https://www.blueseas.com/resources/108/Electrical Conductivity of Materials](https://www.blueseas.com/resources/108/Electrical-Conductivity-of-Materials).
5. Brass 360 Product Guide from Online Metals. (2022) [online] Available at: <https://www.onlinemetals.com/en/product-guide/alloy/360>.
6. Callister, W.D. (2018). Materials science and engineering : an introduction 10E. Hoboken, New Jersey: John Wiley Sons.
7. Chung, D.D.L. (2001). Materials for thermal conduction. Applied Thermal Engineering, [online] 21(16), pp.1593–1605. doi:10.1016/S1359-4311(01)00042-4.
8. Cengel, Y.A. and Ghajar, A.J. (2015). Heat and mass transfer : fundamentals applications. 5th Ed. New York McGraw-Hill Education Cop.
9. Engineering ToolBox (2019). Thermal Conductivity of Metals, Metallic Elements and Alloys. [online] Engineeringtoolbox.com. Available at: <https://www.engineeringtoolbox.com/thermal-conductivity-metals-d858.html>.
10. Ozis, M.N. and Tzou, D.Y. (1994). On the Wave Theory in Heat Conduction. Journal of Heat Transfer, 116(3), pp.526–535. doi:10.1115/1.2910903.
11. Pasco Heat Conduction Apparatus TD-8513. (2022). [online] Available at: <https://cdn.pasco.com/productdocument/Heat-Conduction-Apparatus-Manual-TD-8513.pdf> [Accessed 29 May 2022].

Appendix

Mathematical process was not included for Equation 1 and 2 due to the use of MATLAB 2022ra. Mathematical procedures can be acquired via contact of the author if required for experimental reproduction. However the values used for Equation 1 and 2 can be found in Table 1 and Figure 4. Robert Hawken, rch003@student.usc.edu.au